Type of the manuscript "Original Research Article"

Infrared Spectroscopic Study of $Cs_2Ni(XO_4)_2 \cdot 6H_2O$ (X = S, Se) and of NH_4^+ Ions Included in $M_2Ni(XO_4)_2 \cdot 6H_2O$ (M = Rb, Cs; X = S, Se), and Crystal Structures of $(M, NH_4)_2Ni(XO_4)_2 \cdot 6H_2O$ (M = Rb, Cs; X = S, Se) Mixed Crystals

Veronika Karadjova [1], Manfred Wildner [2] and Donka Stoilova [3*]

[1]*Department of Inorganic Chemistry, University of Chemical Technology and Metallurgy, 8 Kliment Ohridski, 1756 Sofia, Bulgaria.*
[2]*Universität Wien, Geozentrum, Institut für Mineralogie und Kristallographie, Althanstr. 14, A-1090 Wien, Austria.*
[3]*Institute of General and Inorganic Chemistry, Bulgarian Academy of Sciences, 1113 Sofia, Bulgaria.*
stoilova@svr.igic.bas.bg, ***stoilova@svr.igic.bas.bg***

Corresponding author: Email: stoilova@svr.igic.bas.bg

.

ABSTRACT

The solubility in the three-component Cs_2SO_4–$NiSO_4$–H_2O system was studied at 25 °C. It has been established that a double salt, $Cs_2Ni(SO_4)_2 \cdot 6H_2O$, crystallizes within a wide concentration range. Infrared spectra of neat Tutton compounds $Cs_2Ni(XO_4)_2 \cdot 6H_2O$ (X = S, Se) as well as those of ammonium doped rubidium and cesium sulfate and selenate matrices are presented and discussed with respect to the normal modes of the tetrahedral ions and water librations. The ammonium ions included in the sulfates exhibit three bands corresponding to the asymmetric bending modes ν_4 in agreement with the low site symmetry C_1 of the host cesium and rubidium cations. However, the inclusion of ammonium ions in the rubidium and cesium selenates leads to the appearance of four bands in the region of ν_4. At that stage of our knowledge we assume that some kind of disorder of the ammonium ions included in the selenates occurs due to the strong proton acceptor capability of the SeO_4^{2-} (stronger than that of SO_4^{2-}), thus facilitating the formation of polyfurcate hydrogen bonds by the ammonium ions in the selenate matrices. The strength of the hydrogen bonds formed in the mixed crystals $M_{1.85}(NH_4)_{0.15}Ni(XO_4)_2 \cdot 6H_2O$ (M = Rb, Cs; X = S, Se) as deduced from the frequencies of the water librations is discussed. The spectroscopic experiments reveal that the water molecules in the mixed crystals form weaker hydrogen bonds than those in the neat rubidium and cesium Tutton salts due to decreasing in the proton acceptor strength of the SO_4^{2-} and SeO_4^{2-} ions as a result of the formation of hydrogen bonds between the host anions and the NH_4^+ guest cations (*anti*-cooperative or proton acceptor competitive effect). Crystal structure investigations of several $(M,NH_4)_2Ni(XO_4)_2 \cdot 6H_2O$ (M = Rb, Cs; X = S, Se) mixed crystals reveal significant changes in the environment of the monovalent cations as well as in the hydrogen bonding systems of the water molecules upon incorporation of ammonium ions. Disorder of NH_4 groups and the formation of polyfurcate N–H···O hydrogen bonds have not been observed, but neither can be excluded by the X-ray diffraction

* Tel.: +xx xx 265xxxxx; fax: +xx aa 462xxxxx.
E-mail address: xyz@abc.com.

experiments, especially not for rather low ammonium contents.

Keywords: Tutton compounds, $Cs_2Ni(XO_4)_2{\cdot}6H_2O$ (X = S, Se), solubility diagram, infrared spectra, matrix-isolated NH_4^+ guest ions, water librations, crystal structures.

1. INTRODUCTION

$Cs_2Ni(SO_4)_2{\cdot}6H_2O$ and $Cs_2Ni(SeO_4)_2{\cdot}6H_2O$ belong to a large number of isomorphous compounds with a general formula $M'_2M''(XO_4)_2{\cdot}6H_2O$ (M' = K, NH_4^+, Rb, Cs; M'' = Mg, Fe, Co, Ni, Cu, Zn; X = S, Se) known as Tutton salts. The crystal structures of $Cs_2M(XO_4)_2{\cdot}6H_2O$ (M = Mg, Mn, Fe, Co, Ni, Zn; X = S, Se) determined from single crystal X-ray diffraction data are described in [1,2]. As an example the crystal structures of $Cs_2Ni(SO_4)_2{\cdot}6H_2O$ and $(NH_4)_2Ni(SO_4)_2{\cdot}6H_2O$ are shown in Fig. 1. The crystal structures of these compounds (monoclinic space group $P2_1/a$ (C_{2h}^5)) consist of isolated $[Ni(H_2O)_6]$ octahedra, XO_4 tetrahedra and CsO_n polyhedra (n = 8-10). Three crystallographically different water molecules are coordinated to the Ni^{2+} ions. The polyhedra are linked by hydrogen bonds and Cs^+ cations. The water molecules are asymmetrically hydrogen bonded – the $O_W\cdots O$ bond distances vary in the interval of 2.68-2.82 Å. All atoms are located at general positions C_1 with exception of the divalent metal ions, which lie at centre of inversion C_i.

The present paper continues our infrared spectroscopic investigations of Tutton compounds [3-10]. In previous papers the vibrational behavior of SO_4^{2-} ions incorporated in the crystals of $M'_2M''(SeO_4)_2{\cdot}6H_2O$ (M' = K, NH_4^+, Rb; M'' = Mg, Co, Ni, Cu, Zn) is reported. The influence of different crystal chemical factors and the metal ion nature on the extent of energetic distortion of matrix-isolated sulfate ions was analyzed [3-9]. Special attention has been paid on infrared spectra of NH_4^+ ions included in the crystals of $K_2M(XO_4)_2{\cdot}6H_2O$ (M = Mg, Co, Ni, Cu, Zn; X = S, Se) [3-7].

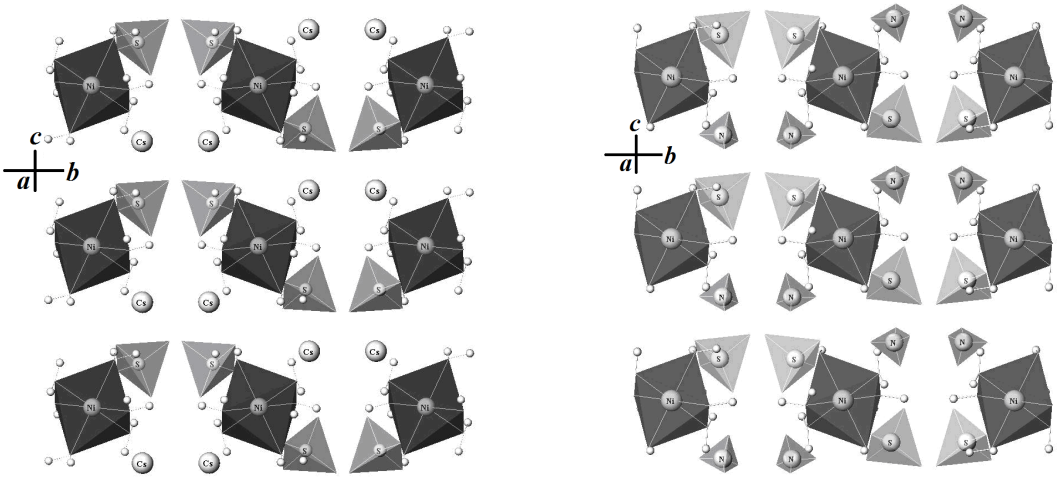

Fig. 1. Crystal structures of $Cs_2Ni(SO_4)_2{\cdot}6H_2O$ and $(NH_4)_2Ni(SO_4)_2{\cdot}6H_2O$ (plane *bc*) according to [2]; small balls – hydrogen atoms of water molecules; the oxygen atoms forming SO_4 tetrahedra, NiO_6 octahedra, CsO_n polyhedra (n = 8-10) and hydrogen atoms forming NH_4 tetrahedra are not shown

In this paper we report our experimental data on the crystallization processes in the ternary Cs_2SO_4–$NiSO_4$–H_2O system at 25 ºC. Fourier transform infrared spectra of the cesium nickel

* Tel.: +xx xx 265xxxxx; fax: +xx aa 462xxxxx.
E-mail address: xyz@abc.com.

double salts, $Cs_2Ni(XO_4)_2 \cdot 6H_2O$ (X = S, Se), are presented and discussed in the regions of the normal vibrations of both the sulfate (selenate) ions and water molecules and the water molecules. A focus has been put on the vibrational behavior of NH_4^+ ions incorporated in the crystals of $M_2Ni(XO_4)_2 \cdot 6H_2O$ (M = Rb, Cs; X = S, Se). The influence of the NH_4^+ guest ions on the strength of the hydrogen bonds formed in the mixed crystals $M_{1.85}(NH_4)_{0.15}Ni(XO_4)_2 \cdot 6H_2O$ (M = Rb, Cs; X = S, Se) as deduced from the wavenumbers of the water librations is commented. In addition, X-ray structure investigations of the ammonium doped compounds were performed on several selected single crystals, in order to provide complementary information about the long range order in these Tutton salt mixed crystals.

2. EXPERIMENTALS

Rb_2SeO_4, Rb_2SO_4, Cs_2SeO_4, Cs_2SO_4, $(NH_4)_2SeO_4$, and $NiSeO_4 \cdot 6H_2O$ were prepared by neutralization of the respective carbonates and nickel hydroxide carbonates with dilute selenic or sulfuric acid solutions at 60−70 ºC. Then the solutions were filtered, concentrated at 40−50 ºC, and cooled to room temperature. The crystals were filtered, washed with alcohol and dried in air. $Rb_2Ni(SO_4)_2 \cdot 6H_2O$ was prepared by crystallization from ternary solutions according to the solubility diagram of the Rb_2SO_4−$NiSO_4$−H_2O system [9]; $Rb_2Ni(SeO_4)_2 \cdot 6H_2O$ – according to the solubility diagram of the Rb_2SeO_4−$NiSeO_4$−H_2O system [10]; $Cs_2Ni(SeO_4)_2 \cdot 6H_2O$ – according to the solubility diagram of the Cs_2SeO_4−$NiSeO_4$−H_2O system [11]; $Cs_2Ni(SO_4)_2 \cdot 6H_2O$ – according to the solubility diagram of the Cs_2SO_4−$NiSO_4$−H_2O system (this paper). The samples of $M_{2-x}(NH_4)_xNi(XO_4)_2 \cdot 6H_2O$ (M = Rb, Cs; X= S, Se; x = 0.02, 0.05, 0.10 and 0.15) were prepared by crystallization from the above ternary selenate (sulfate) solutions in the presence of different amounts of ammonium ions. All reagents used were of reagent grade quality (Merck).

The solubility in the three-component system Cs_2SO_4−$NiSO_4$−H_2O was studied by the method of isothermal decrease of supersaturation described in [12]. Solutions containing different amounts of the salt compounds corresponding to each point of the solubility isotherm were heated at about 60-70 °C and cooled to room temperature. Then the saturated solutions containing solid phases were vigorously stirred. The equilibrium between the liquid and solid phases was reached in about 20 hours. The analysis of the liquid and wet solid phases was performed, as follows: the nickel ion contents were determined complexonometrically at pH 5.5-6 using xylenol orange as indicator; the sulfate ions were determined gravimetrically as $BaSO_4$; the concentrations of the cesium sulfate were calculated by difference. The compositions of the solid phases were identified by means of X-ray diffraction and infrared spectroscopy methods as well.

The infrared spectra were recorded on a Bruker model IFS 25 Fourier transform interferometer (resolution < 2 cm^{-1}) at ambient temperature using KBr discs as matrices. Ion exchange or other reactions with KBr have not been observed. The X-ray powder diffraction patterns were collected within the range from 5° to 50° 2 θ with a step 0.02° 2 θ and counting time 35 s/step on Bruker D8 Advance diffractometer with Cu Kα radiation and LynxEye detector.

Suitable individual crystals for single crystal structure investigations of the prepared ammonium doped Tutton compounds, $M_{2-x}(NH_4)_xNi(XO_4)_2 \cdot 6H_2O$ (M = Rb, Cs; X = S, Se; x = 0.02, 0.05, 0.10 and 0.15; see above), were hand-picked according to optical quality from those synthesis products with higher bulk ammonium contents (i.e. x = 0.10 and 0.15). X-ray diffraction data of these eight selected single crystals were measured at room temperature using graphite monchromatized MoKα radiation on a Nonius Kappa-CCD diffractometer equipped with an X-ray capillary optics collimator. For each crystal several sets of φ- and ω-

* Tel.: +xx xx 265xxxxx; fax: +xx aa 462xxxxx.
E-mail address: xyz@abc.com.

scans with 2° rotation per CCD-frame were performed to collect the complete Ewald sphere up to 2θ = 80° at a crystal to detector distance of 30 mm. The extraction and correction of the intensity data, merging of redundant data to hkl's, a pseudo-absorption correction by frame scaling, and the refinement of the lattice parameters were done with the program DENZO-SMN [13].

Structure refinements on F^2 with scattering curves for neutral atoms were performed with SHELXL-97 [14], each refinement including hydrogen atoms of the water molecules, anisotropic displacement parameters of the non-hydrogen atoms, as well as a site occupancy parameter for the nitrogen atom of the ammonium group replacing Rb or Cs (assuming a total site occupancy of 1). Atom labels and equivalent site positions were selected as in [15]. The results show that the refined NH_4 content in the investigated single crystals clearly exceeds that of the bulk composition, especially in case of the two Rb compounds with the respective higher bulk ammonium content (x = 0.15). This seems to be an "artifact" of the selection of optically clear and flawless single crystals from the bulk products. In detail, the refined ammonium contents y (y to distinguish them from the bulk contents x) for the MN_xX-labelled compounds are y = 0.26 ($RbN_{0.10}S$), 0.40 ($RbN_{0.15}S$), 0.22 ($CsN_{0.10}S$), 0.28 ($CsN_{0.15}S$), 0.14 ($RbN_{0.10}Se$), 0.99 ($RbN_{0.15}Se$), 0.17 ($CsN_{0.10}Se$), and 0.26 ($CsN_{0.15}Se$). As a beneficial effect of the high ammonium content y = 0.99 of the $RbN_{0.15}Se$ crystal, we were able to find positions of the hydrogen atoms of the NH_4 group in difference Fourier maps, and to refine them applying soft restraints and a common isotropic displacement parameter. NH_4 hydrogen positions and labels HN1-4 correspond to H(11)-H(14) of Montgomery [16]. Subsequently, we surprisingly even succeeded to spot respective difference Fourier peaks for the crystal with the second highest refined ammonium content (y = 0.40 for $RbN_{0.15}S$), and refined them in the same way. In all other cases, difference Fourier peaks surrounding Rb or Cs sites were not considered as potential partially occupied hydrogen positions due to the extreme discrepancy in X-ray scattering power. Table 2 summarizes crystal data and details of the data collections and structure refinements for the compounds with the respective higher bulk ammonium content (x = 0.15). Corresponding final atomic coordinates and equivalent (H: isotropic) displacement parameters are listed in Table 3. Anisotropic displacement parameters of the non-hydrogen atoms and structural data of the other compounds (x = 0.10) can be obtained from the second author upon request.

2. RESULTS AND DISCUSSION

3.1 Solubility diagram of the three-component system Cs_2SO_4–$NiSO_4$–H_2O at 25 ºC

The solubility diagram of the three-component system Cs_2SO_4−$NiSO_4$−H_2O is shown in Fig. 2. The experimental solubility data are listed in Table 1. Three crystallization fields are observed in the solubility diagram – a very narrow crystallization field of Cs_2SO_4, a comparatively large crystallization field of $NiSO_4{\cdot}7H_2O$ and a remarkably wide crystallization field of a double salt with composition $Cs_2Ni(SO_4)_2{\cdot}6H_2O$. The composition of the double compound is proved by chemical analysis and X-ray powder diffraction measurements. The experimental results show that small amounts of nickel sulfate added into the cesium sulfate solution lead to the formation of the double salt. The large width of the double salts crystallization field indicates that strong complex formation processes occur in the ternary solutions. $Cs_2Ni(SO_4)_2{\cdot}6H_2O$ crystallizes from solutions containing 62.84 mass% cesium sulfate and 0.87 mass% nickel sulfate up to solutions containing 10.85 mass% cesium sulfate and 29.62 mass% nickel sulfate (eutonic points). The X-ray powder diffraction patterns as well as the calculated lattice parameters of the samples obtained from the crystallization field of the double salts coincide well with those reported in [2].

* Tel.: +xx xx 265xxxxx; fax: +xx aa 462xxxxx.
E-mail address: xyz@abc.com.

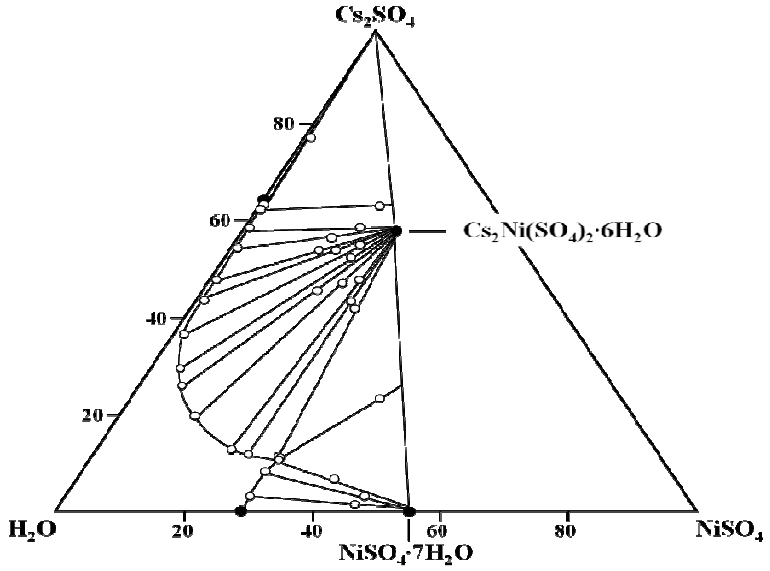

Fig. 2. Solubility diagram of the system Cs_2SO_4–$NiSO_4$–H_2O at 25 °C

Table 1. Solubility in the Cs_2SO_4–$NiSO_4$–H_2O system at 25 °C

Liquid phase, mass%		Wet solid phase, mass%		Composition of the solid phases
Cs_2SO_4	$NiSO_4$	Cs_2SO_4	$NiSO_4$	
64.88	-	-	-	Cs_2SO_4
63.86	0.96	77.39	1.46	" – "
62.84	0.87	63.15	19.38	Cs_2SO_4 + $Cs_2Ni(SO_4)_2·6H_2O$
58.72	1.03	58.79	18.31	$Cs_2Ni(SO_4)_2·6H_2O$
54.18	1.12	56.64	15.11	" – "
43.82	1.14	54.19	17.16	" – "
41.67	0.94	55.03	20.05	" – "
26.84	6.91	45.62	17.85	" – "
14.28	20.11	48.06	23.85	" – "
12.13	24.31	43.59	24.91	" – "
11.94	28.74	42.02	26.04	" – "
10.85	29.62	23.57	39.24	$NiSO_4·7H_2O$ + $Cs_2Ni(SO_4)_2·6H_2O$
10.47	29.73	6.85	30.52	$NiSO_4·7H_2O$
8.56	28.87	3.88	46.43	" – "
3.35	29.88	1.83	46.37	" – "
-	29.04	-	-	" – "

3.2 Infrared spectra of neat cesium Tutton compounds, $Cs_2Ni(SO_4)_2·6H_2O$ and $Cs_2Ni(SeO_4)_2·6H_2O$

The free tetrahedral ions (XO_4^{n-}) under perfect T_d symmetry exhibit four internal vibrations: $\nu_1(A_1)$, the symmetric X–O stretching modes, $\nu_2(E)$, the symmetric XO_4 bending modes, $\nu_3(F_2)$ and $\nu_4(F_2)$, the asymmetric stretching and bending modes, respectively. The normal

* Tel.: +xx xx 265xxxxx; fax: +xx aa 462xxxxx.
E-mail address: xyz@abc.com.

vibrations of the free tetrahedral ions in aqueous solutions are reported to appear, as follows: for the selenate ions – ν_1 = 833 cm^{-1}, ν_2 = 335 cm^{-1}, ν_3 = 875 cm^{-1}, ν_4 = 432 cm^{-1}; for the sulfate ions – ν_1 = 983 cm^{-1}, ν_2 = 450 cm^{-1}, ν_3 = 1105 cm^{-1}, ν_4 = 611 cm^{-1}; for the ammonium ions – ν_1 = 3040 cm^{-1}, ν_2 = 1680 cm^{-1}, ν_3 = 3145 cm^{-1}, ν_4 = 1400 cm^{-1} [17]. On going into solid state, the normal modes of the XO_4^{2-} (X = S, Se) ions are expected to shift to higher or lower frequencies.

The monoclinic unit cell of the cesium nickel compounds (Z = 2; factor group symmetry C_{2h}) contains 62 atoms with 186 zone-centre degrees of freedom. The 186 vibrational modes of the unit cell decompose according to the following representation:

Γ = 45Ag + 45Bg + 48Au + 48Bu, where 1Au + 2Bu are translations (acoustic modes).

Since the crystal structures are centrosymmetric, the Raman modes display *g*-symmetry, and their infrared (IR) counterparts display *u*-symmetry (mutual exclusion principle). The XO_4^{2-} ions (four XO_4^{2-} ions in the unit cell located on C_1 sites) and the water molecules (twelve molecules in the unit cell located on C_1 sites) contribute 72 internal modes to the 183 optical zone-centre modes – each tetrahedral ion is characterized with nine normal vibrations and each water molecule with three normal vibrations, i.e. 36 internal modes for the tetrahedral ions and 36 internal modes for the water molecules. The static field (related to the low symmetry C_1 of the sites on which the XO_4^{2-} ions are situated) will cause a removal of the degeneracy of both the doubly degenerate ν_2 modes and the triply degenerate ν_3 and ν_4 modes (the non-degenerate ν_1 mode is activated). The nine internal modes of the tetrahedral ions are of A symmetry as predicted from the site group analysis: one mode for the symmetric stretching vibrations (ν_1), two modes for the symmetric bending vibrations (ν_2), and three modes for both asymmetric stretching and bending vibrations (ν_3 and ν_4). Additionally, under the factor group symmetry C_{2h} each species of A symmetry split into four components – A_g + B_g + A_u + B_u (related to interactions of identical oscillators, correlation field effect, see Fig. 3). The remaining 111 optical modes (external modes) are distributed between the translational and librational lattice modes. Thus, the unit cell theoretical treatment for the translational lattice modes (Cs^+, XO_4^{2-}, $H_2O(1)$, $H_2O(2)$, and $H_2O(3)$ – all in C_1 site symmetry, Ni^{2+} – in C_i site symmetry) and librational lattice modes (XO_4^{2-}, $H_2O(1)$, $H_2O(2)$, and $H_2O(3)$) yields: 63 translations ($15A_g$ + $15B_g$ + $17A_u$ + $16B_u$) and 48 librations ($12A_g$ +$12B_g$ + $12A_u$ + $12B_u$).

The literature data concerning infrared spectroscopic investigations of the cesium nickel Tutton salts are scanty [18,19]. Our experimental results are presented in Fig. 4 (spectral interval 4000−400 cm^{-1}). The six infrared bands expected for ν_3 of the SO_4^{2-} ions according to the factor group analysis coalesce into three bands – 1134, 1113 and 1098 cm^{-1}. The weak band at 981 cm^{-1} results from the symmetric stretching modes ν_1. If we assigned the three components of ν_3 as ν_{3a}, ν_{3b} and ν_{3c} (ν_{3a} appears at the highest frequency and ν_{3c} – at the lowest frequency), the differences $\Delta\nu_{ab}$, $\Delta\nu_{bc}$ and $\Delta\nu_{ac}$ have values of 21, 15, and 36 cm^{-1}, respectively. These differences are too large to be accepted as a result of the factor group splitting and consequently the three infrared bands at 1134, 1113 and 1098 cm^{-1} are assigned to the three site group components of ν_3. The asymmetric bending motions ν_4 of the sulfate ions appear as a doublet – bands at 630 and 619 cm^{-1}. The spectroscopic measurements show that the difference between the frequencies of the asymmetric bending vibrations have a value of 11 cm^{-1} (i.e. smaller than that for the asymmetric stretching vibrations ν_3), thus indicating that the sulfate tetrahedra are smaller energetically distorted with respect to the O−S−O bond angles as compared to the S−O bond lengths. A strong band centered at 880 cm^{-1} in the spectrum of the cesium nickel selenate results from the asymmetric stretching motions ν_3 of the selenate ions (correspondingly ν_1 is observed at 833

* Tel.: +xx xx 265xxxxx; fax: +xx aa 462xxxxx.
E-mail address: xyz@abc.com.

cm^{-1}) (see Fig. 4). The appearance of one band only corresponding to ν_3 instead of three bands expected according to the site group analysis indicate that the *effective* spectroscopic symmetry of the selenate ions is close to T_d (at least at ambient temperature). The bands at 429 and 406 cm^{-1} arise from the symmetric bending modes ν_4. The other components of ν_4 as well the symmetric bending modes ν_2 appear at frequencies lower than 400 cm^{-1}.

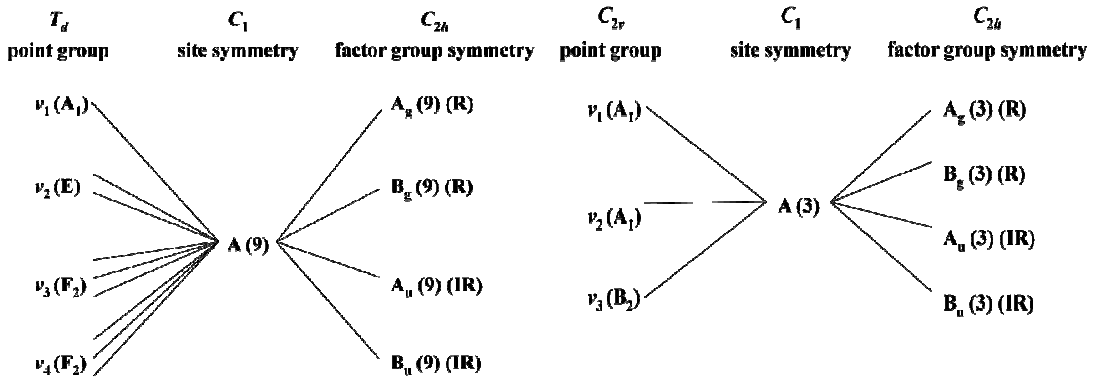

Fig. 3. Correlation diagrams between: T_d point symmetry, C_1 site symmetry and C_{2h} factor group symmetry (XO_4^{2-} ions; X = S, Se) (left side); C_{2v} point symmetry, C_1 site symmetry and C_{2h} factor group symmetry (water molecules) (right side)

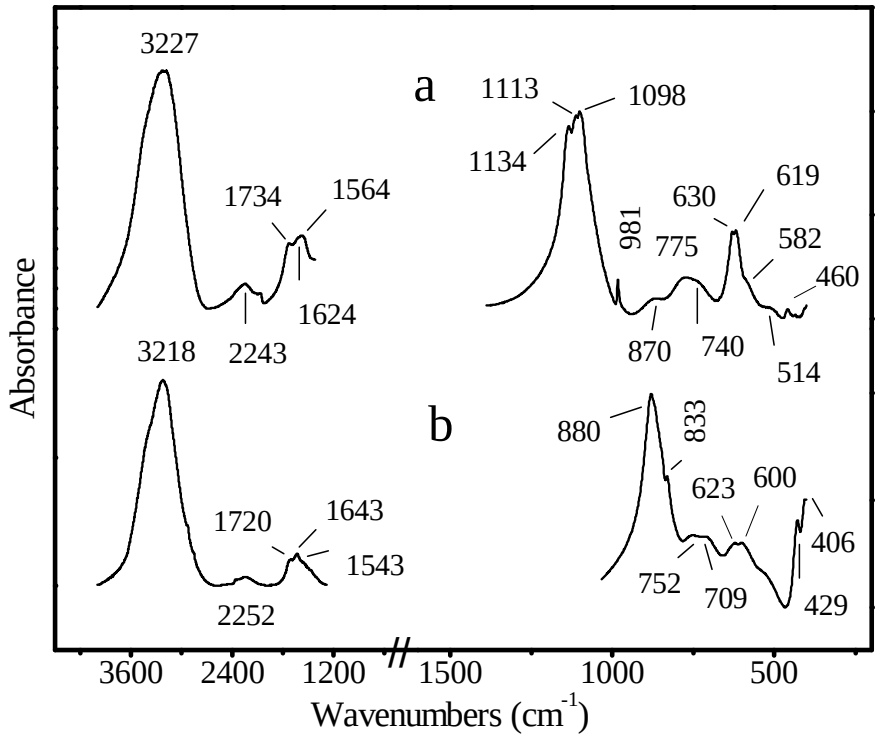

Fig. 4. Infrared spectra of neat Tutton salts $Cs_2Ni(XO_4)_2 \cdot 6H_2O$ (X =S, Se) in the region of 4000−400 cm^{-1} (a, cesium sulfate; b, cesium selenate)

* Tel.: +xx xx 265xxxxx; fax: +xx aa 462xxxxx.
E-mail address: xyz@abc.com.

According to Petruševski and Šoptrajanov [20] the intensity of the bands corresponding to ν_1 reflects the degree of distortion of the sulfate ions in a series of salts – the higher the intensity of these bands is the stronger the distortion of the polyatomic ions is. Thus, the very small intensity of the band at 981 cm^{-1} (Fig. 4a) is an indication that the sulfate tetrahedra in the nickel sulfate are slightly distorted with respect to the S−O bond lengths in good agreement with the structural data − $\Delta r(XO_4)$ has a value of 0.019 Å ($\Delta r(XO_4)$ is the difference between the longest and the shortest S–O bond lengths in the sulfate tetrahedron [2]). Fig. 4b shows that the band corresponding to the ν_1 in the spectrum of the respective selenate is of a higher intensity than expected if the geometric distortion of the selenate tetrahedra are concerned ($\Delta r(SeO_4)$ has a value of 0.016 Å [1]). This fact is due to some coupling of the symmetric and asymmetric motions of the selenate ions which occur in a very close spectral interval.

Our infrared spectroscopic measurements differ slightly from those reported by Brown and Ross [18] with respect to the number of the bands corresponding to ν_3 of the sulfate and selenate ions (more components of ν_3 are reported in that paper – some of them assigned as shoulders; however, the spectra are not shown). One of the reason for the difference between our spectra and those reported by Brown and Ross could be the temperature at which the spectra are recorded (it is mentioned in [18] that some spectra are run at liquid nitrogen temperature (LNT); however, there is no indication which ones are obtained at liguid nitrogen temperature). The second reason could be the conditions under which the spectra are obtained. The spectra of the selenates commented in [18] are recorded in Nujol mulls. It is well known that in this case the halfwidths of the bands are larger (the appearance of the shoulders is not unexpected) as compared to those of the bands in the spectra obtained when the pellets of KBr are used.

The three crystallographically different water molecules (each water molecule in C_1 site symmetry) exhibit three sets of normal vibrations of the water molecules – ν_3, ν_2 and ν_1. So, the stretching modes (ν_3 and ν_1) are expected to display six infrared bands in the high frequency region in absence of correlation field effects. However, comparatively broad and intensive bands centered at 3227 and 3218 cm^{-1} for the sulfate and selenate, respectively, are observed in the spectra (see Fig. 4) owing to the strong interactions of the identical oscillators O−H. It is readily seen from Fig. 4 that slightly weaker hydrogen bonds occur in the cesium nickel sulfate (ν_{OH} appears at higher frequencies) than those formed in the respective selenate due to the weaker proton acceptor ability of the sulfate ions [21-27]. As far as the weak broad bands at 2243 cm^{-1} (sulfate) and 2252 cm^{-1} (selenate) are concerned, they result probably from second-order transitions (combinations of bending modes of the water molecules and some librations of the same species).

The infrared spectra display three bands in the region of ν_2 (some of the bands appear as shoulders), as follows: $Cs_2Ni(SO_4)_2{\cdot}6H_2O$ – 1734, 1624 and 1564 cm^{-1} and $Cs_2Ni(SeO_4)_2{\cdot}6H_2O$ − 1720, 1643 and 1543 cm^{-1} (see Fig. 4a and b, respectively). Šoptrajanov and Petruševski [28] reported that complex spectral pictures are observed in the infrared spectra of Tutton compounds, $M'_2M''(XO_4)_2{\cdot}6H_2O$ (M' = K, Rb; M'' = Mg, Fe, Co, Ni, Cu; X = S, Se), in the region of the water bending modes. They established that complex spectra appear always irrespective of the type of the univalent and divalent cations and of the type of the anions (sulfate and selenate). According to the authors the differences in the band frequencies extend over the region of hundreds of wavenumbers and the origin of such complex spectra could not be explained with the structural differences between the three crystallographically different water molecules. They claim that vibrational interactions between the bending modes ν_2 and overtones or combinations arising from water librations

* Tel.: +xx xx 265xxxxx; fax: +xx aa 462xxxxx.
E-mail address: xyz@abc.com.

(especially those which appear in the 900–700 cm^{-1} region, rocking modes) are responsible for the complex spectral pictures.

The water librations (rocking, twisting and wagging) appear in the region below 1000 cm^{-1} and a strong overlapping of the water librations with vibrations of other entities in the structure is expected. Two types of water librations for the Tutton sulfates (potassium and ammonium) are discussed in the literature – rocking and wagging, the former observed at higher frequencies [19]. Each type is characterized with two broad bands. The water molecules bonded to the M'' ions via shorter M''–OH_2 bonds display water librations at higher frequencies as compared to those forming longer M''–OH_2 bonds (equatorial water molecules). The former M''–OH_2 bonds are much more polarized due to the stronger synergetic effect of the M'' ions (stronger metal-water interactions). The mean wavenumbers for the rocking librations are reported to have values of 855 and 740 cm^{-1}, and 770 and 680 cm^{-1} for the potassium and ammonium sulfates, respectively. The respective wagging modes are reported to have mean values of 570 and 441 cm^{-1} for the potassium compounds, and 544 and 425 cm^{-1} for the ammonium ones [19].

The assignments of the bands originated from the water librations are performed according to Refs. [29-31]. Two well distinguished groups of infrared bands are seen in the spectrum of the selenate (the first at 752 and 709 cm^{-1}, and the second at 623 and 600 cm^{-1}) which are attributed to rocking and wagging modes of the two types of the water molecules, respectively (these librations are free from motions of other entities in the structure, see Fig. 4b). The bands at 870, 775 and 740 cm^{-1} result from rocking modes of the water molecules in the sulfate (Fig. 4a). However, the wagging modes (shoulders at about 582 and 520 cm^{-1}) in the sulfate structure are probably strongly influenced by the bending vibrations of the sulfate ions, especially those which occur at higher frequencies and the wavenumbers of the respective bands could not be recognized well.

3.3 Infrared spectra of NH_4^+ ions included in $M_2Ni(XO_4)_2{\cdot}6H_2O$ (M = Rb, Cs; X = S, Se)

Infrared spectra of mixed crystals $M_{2-x}(NH_4)_xNi(XO_4)_2{\cdot}6H_2O$ (M = Rb, Cs; X = S, Se) are presented in Figs. 5 (infrared spectra of the ammonium salts are taken from [7]; those of the rubidium ones from [9,10]). The experimental results show differences in the vibrational behavior of the ammonium ions included in both matrices. The ammonium ions included in the sulfate matrix exhibit three bands corresponding to the asymmetric bending modes ν_4 of the ammonium ions in agreement with the low site symmetry C_1 of the host rubidium and cesium ions (1472, 1433 and 1402 cm^{-1} in the $Rb_2Ni(SO_4)_2{\cdot}6H_2O$ matrix and 1467, 1441 and 1402 cm^{-1} in the $Cs_2Ni(SO_4)_2{\cdot}6H_2O$ matrix). However, the inclusion of ammonium ions in the selenate matrices leads to the appearance of four bands in the region of ν_4 (bands at 1463, 1439, 1422 and 1400 cm^{-1} in the rubidium nickel selenate, and bands at 1464, 1444, 1421 and 1402 cm^{-1} in the cesium nickel selenate (x ~ 0.10 and x ~ 0.15), respectively). Ammonium ions included in the crystals of potassium Tutton selenates exhibit the same behavior [3-7].

It is reported that some kind of disorder of the ammonium ions occurs in the crystal structures of the ammonium salts when these ions exhibit a coordination number larger than 5 as a result of the formation of di- or polyfurcate hydrogen bonds [32,33]. For example, the appearance of four bands corresponding to the bending modes of NH_3D^+ ions included in struvite-type compounds instead of three bands expected is commented in terms of disorder of the ammonium ions [34-36]. Cahil *et al*. [37] claim that even in the cases when three bands only are observed a disorder of the ammonium ions is not excluded. So, at that stage of our knowledge we assume that some kind of disorder of the ammonium ions included in the selenate lattices occurs. However, the origin of these bands is open to discussion. In our

* Tel.: +xx xx 265xxxxx; fax: +xx aa 462xxxxx.
E-mail address: xyz@abc.com.

opinion the observed difference in the vibrational behavior of the NH_4^+ guest ions included in the selenate and sulfate structures is due to the different proton acceptor strength of the SO_4^{2-} and SeO_4^{2-} ions (as was commented above in the text the selenate ions exhibit stronger proton acceptor abilities than the sulfate ones). This fact will facilitate the formation of polyfurcate hydrogen bonds in the selenate matrices, thus leading to an increase in the coordination number of the ammonium ions, i.e. to a disorder of the guest ions.

Furthermore, the spectroscopic experiments show that the four bands corresponding to ν_4 of the ammonium ions included in the rubidium selenate matrix appear at lower concentrations (about 2 mol%) as compared to those of the same ions included in the cesium selenate matrix (the lowest wavenumbered band at 1402 cm^{-1} appears at concentrations of ammonium ions of about 10 mol%) (see Fig. 5).

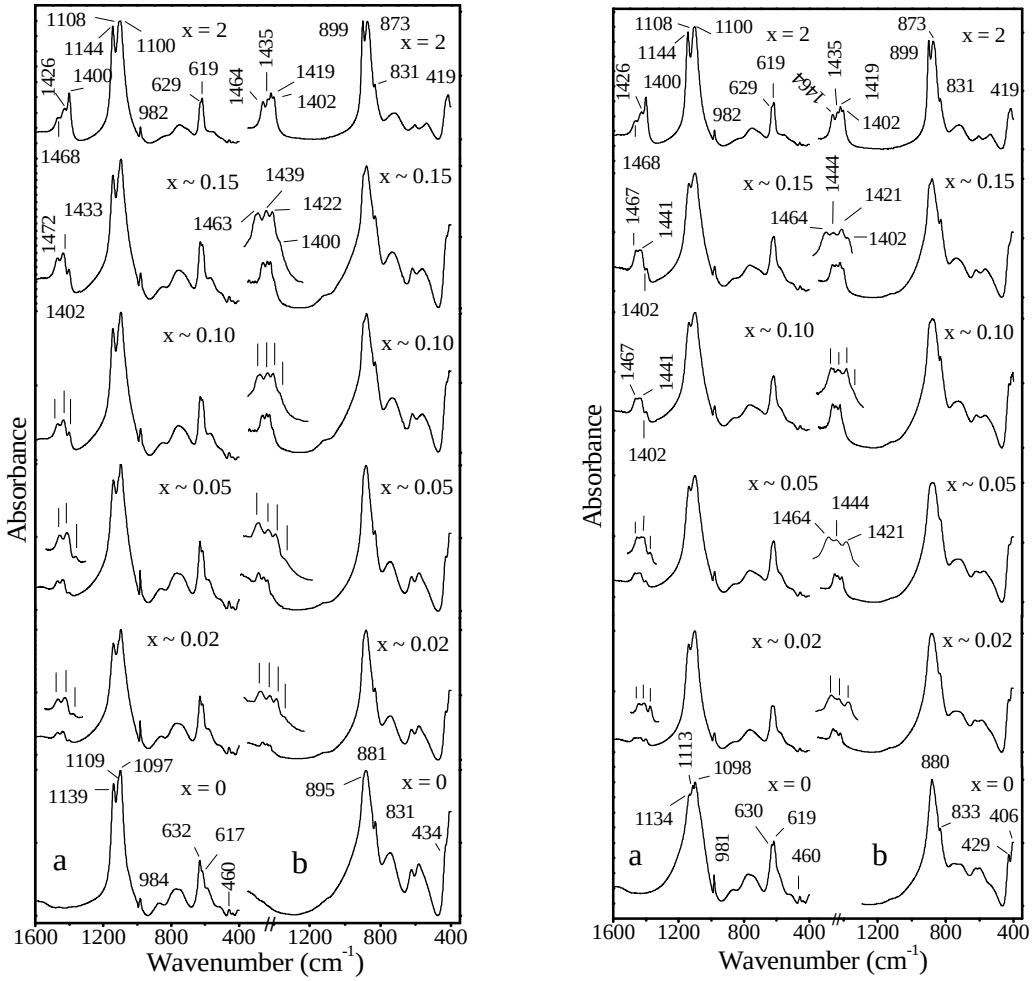

Fig. 5. Infrared spectra of: neat Tutton salts $Rb_2Ni(XO_4)_2 \cdot 6H_2O$, $(NH_4)_2Ni(XO_4)_2 \cdot 6H_2O$ (X = S, Se) and of mixed crystals $Rb_{2-x}(NH_4)_xNi(XO_4)_2 \cdot 6H_2O$ (left side); neat Tutton salts $Cs_2Ni(XO_4)_2 \cdot 6H_2O$, $(NH_4)_2Ni(XO_4)_2 \cdot 6H_2O$ (X = S, Se) and of mixed crystals $Cs_{2-x}(NH_4)_xNi(XO_4)_2 \cdot 6H_2O$ (right side) (*x* is approximately 0.02, 0.05, 0.10, 0.15) in the region of ν_3 and ν_1 of the XO_4^{2-} ions, ν_4 of NH_4^+ ions and water librations (a, sulfates; b, selenates)

* Tel.: +xx xx 265xxxxx; fax: +xx aa 462xxxxx.
E-mail address: xyz@abc.com.

Fig. 6 shows spectra of the neat rubidium and cesium compounds and those of the mixed crystals $Rb_{1.85}(NH_4)_{0.15}Ni(XO_4)_2 \cdot 6H_2O$ and $Cs_{1.85}(NH_4)_{0.15}Ni(XO_4)_2 \cdot 6H_2O$ (X = S, Se) in the region of the water librations. It is readily seen that the bands arising from the water librations in the mixed crystals broaden and shift to lower frequencies, thus indicating that weaker hydrogen bonds are formed in the mixed crystals as compared to those formed in the neat rubidium and cesium compounds (it is well known that the water librations appear at lower frequencies in the case of weaker hydrogen bonds [23,27]). The formation of weaker hydrogen bonds by the water molecules in the mixed crystals is due to the decrease in the proton acceptor capacity of the SO_4^{2-} and SeO_4^{2-} anions, since these ions are involved in hydrogen bonds with the NH_4^+ guest ions additionally to water molecules (*anti*-cooperative or proton acceptor competitive effect) [27 and Refs. therein].

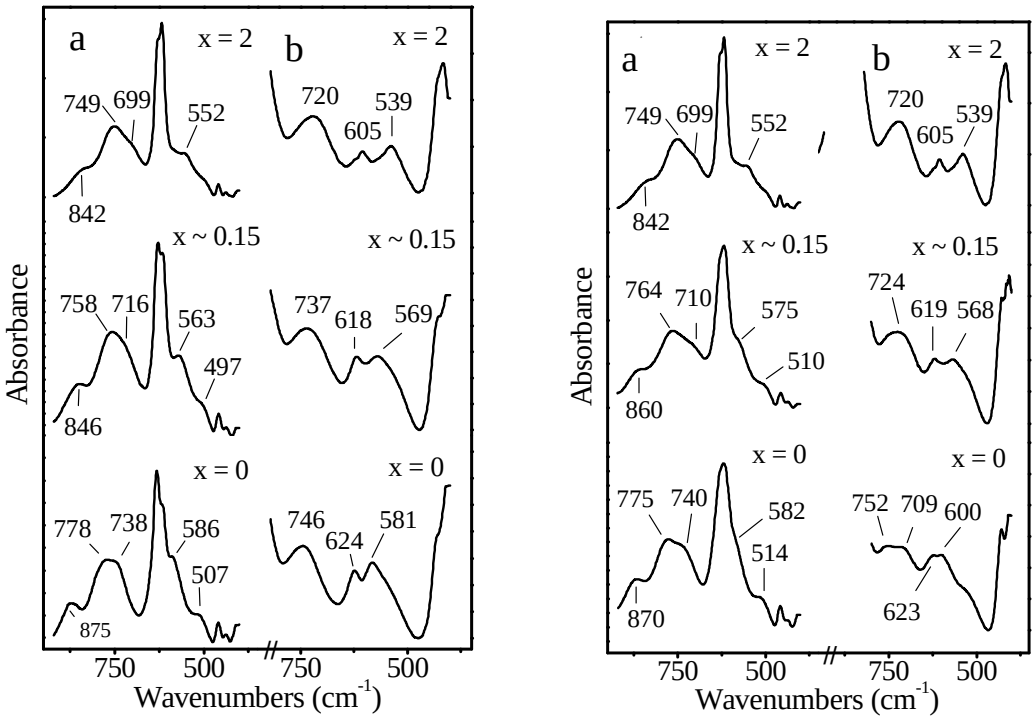

Fig. 6. Infrared spectra of: neat Tutton compounds $Rb_2Ni(XO_4)_2 \cdot 6H_2O$, $(NH_4)_2Ni(XO_4)_2 \cdot 6H_2O$ (X = S, Se), and of mixed crystals of $Rb_{1.85}Ni(NH_4)_{0.15}(XO_4)_2 \cdot 6H_2O$ (left side); $Cs_2Ni(XO_4)_2 \cdot 6H_2O$, $(NH_4)_2Ni(XO_4)_2 \cdot 6H_2O$ (X = S, Se), and of mixed crystals $Cs_{1.85}Ni(NH_4)_{0.15}(XO_4)_2 \cdot 6H_2O$ (right side) in the region of water librations (a, sulfates; b, selenates)

3.4 Crystal structures of $(M,NH_4)_2Ni(XO_4)_2 \cdot 6H_2O$ mixed crystals (M = Rb, Cs; X = S, Se)

The experimental results obtained from crystal structure investigations are listed in Tables 2-5. As was commented above in the text Table 2 summarizes crystal data and details of the data collections and structure refinements for the compounds with the respective higher bulk ammonium content (x = 0.15). Corresponding final atomic coordinates and equivalent (H: isotropic) displacement parameters are listed in Table 3.

* Tel.: +xx xx 265xxxxx; fax: +xx aa 462xxxxx.
E-mail address: xyz@abc.com.

Table 2. Crystal data and details of X-ray data collections and structure refinements for selected single crystals (see text) of ammonium-doped Tutton compounds $M_{2-y}(NH_4)_yNi(XO_4)_2 \cdot 6H_2O$ (M = Rb, Cs; X = S, Se)

MX	RbS	CsS	RbSe	CsSe
refined y (NH_4)	0.395(4)	0.275(4)	0.991(5)	0.259(3)
crystal system, space group, Z	monoclinic, $P2_1/a$ (No. 14), Z = 2			
a (Å)	9.146(2)	9.262(2)	9.315(2)	9.432(2)
b (Å)	12.428(2)	12.733(2)	12.621(2)	12.899(2)
c (Å)	6.232(1)	6.351(1)	6.359(1)	6.464(1)
β (°)	106.23(1)	107.12(1)	105.85(1)	106.34(1)
V (Å^3)	680.1(2)	715.7(2)	719.2(2)	754.7(2)
μ (mm^{-1})	7.5	6.0	9.9	10.3
D_{calc} (g cm^{-3})	2.457	2.750	2.571	3.029
$2\theta_{max}$		80		
exposure time (s) / frame	2×20	2×18	2×20	2×40
CCD frames measured	513	487	496	498
frame scale factors $_{min\ /\ max}$	0.69 / 1.10	0.85 / 1.24	0.46 / 1.25	0.19 / 1.13
total number of intensity data	45940	44857	47682	53816
intensity data for unit cell	14665	17046	15901	27093
number of reflections	34093	30596	34200	32121
number of hkl's	15981	15509	16546	16694
unique hkl's	4198	4405	4449	4632
$F_o > 4\sigma(F_o)$	3162	3390	3335	3779
R_i (%)	4.56	3.61	5.23	3.20
variables	128	115	128	115
wR2 [for all F_o^2] (%)	5.97	5.62	7.22	5.35
R1 [for $F_o > 4\sigma(F_o)$] (%)	3.04	2.57	3.23	2.41
R1 [for all F_o] (%)	5.28	4.45	5.58	3.64
goodness of fit	0.98	1.07	1.03	1.05
weighting[1] parameter a / b	0.022 / 0.20	0.018 / 0.30	0.030 / 0.25	0.018 / 0.40
extinction coefficient	0.021(1)	0.007(1)	0.008(1)	0.005(1)
$\Delta\rho_{max\ /\ min}$ (eÅ^{-3})	0.48 / -0.39	1.13 / -0.82	0.75 / -0.84	0.78 / -0.73

[1] weighting scheme : $w = 1/[s^2(F_o^2) + (aP)^2 + bP]$; $P = \{[\max of (0 or F_o^2)] + 2F_c^2\} / 3$

Table 3. Atomic coordinates and equivalent (H: isotropic) displacement parameters (Å^2) for selected single crystals (see text) of ammonium-doped Tutton compounds $M_{2-y}(NH_4)_yNi(XO_4)_2 \cdot 6H_2O$ (M = Rb, Cs; X = S, Se). Site occupancy factors (sof) of the NH_4 groups (sof ≡ y/2) are given as well

site	MX	x	y	z	U_{eq} / U_{iso}	sof (NH_4)
M, N	RbS	0.13213(2)	0.34957(1)	0.34813(3)	0.0294(1)	0.198(2)
	CsS	0.13025(1)	0.35348(1)	0.35596(2)	0.0279(1)	0.138(2)
	RbSe	0.13927(4)	0.34338(3)	0.34698(6)	0.0314(1)	0.496(3)
	CsSe	0.13606(1)	0.34924(1)	0.35328(2)	0.0298(1)	0.130(1)
S	RbS	0.40502(3)	0.13877(2)	0.73293(5)	0.0188(1)	
	CsS	0.39841(4)	0.14492(3)	0.74143(6)	0.0192(1)	
Se	RbSe	0.41028(2)	0.13548(1)	0.73692(3)	0.0194(1)	
	CsSe	0.40197(2)	0.14285(1)	0.74343(2)	0.0196(1)	

* Tel.: +xx xx 265xxxxx; fax: +xx aa 462xxxxx.
E-mail address: xyz@abc.com.

Table 3 cont.

Ni	RbS	0	0	0	0.0166(1)
	CsS	0	0	0	0.0171(1)
	RbSe	0	0	0	0.0165(1)
	CsSe	0	0	0	0.0170(1)
O1	RbS	0.4151(1)	0.2311(1)	0.5894(2)	0.0310(2)
	CsS	0.4186(2)	0.2361(1)	0.6097(2)	0.0330(3)
	RbSe	0.4206(2)	0.2353(1)	0.5772(2)	0.0326(3)
	CsSe	0.4238(2)	0.2420(1)	0.5976(2)	0.0354(3)
O2	RbS	0.5453(1)	0.0754(1)	0.7795(2)	0.0373(3)
	CsS	0.5351(1)	0.0800(1)	0.8005(2)	0.0349(3)
	RbSe	0.5628(2)	0.0664(1)	0.7842(3)	0.0447(4)
	CsSe	0.5504(1)	0.0712(1)	0.8022(3)	0.0390(3)
O3	RbS	0.2763(1)	0.0704(1)	0.6117(2)	0.0259(2)
	CsS	0.2712(1)	0.0810(1)	0.6065(2)	0.0274(2)
	RbSe	0.2708(1)	0.0604(1)	0.6070(2)	0.0266(3)
	CsSe	0.2635(1)	0.0733(1)	0.5992(2)	0.0288(2)
O4	RbS	0.3784(1)	0.1778(1)	0.9434(2)	0.0290(2)
	CsS	0.3627(2)	0.1822(1)	0.9416(2)	0.0298(2)
	RbSe	0.3820(2)	0.1801(1)	0.9650(2)	0.0297(3)
	CsSe	0.3642(2)	0.1848(1)	0.9623(2)	0.0299(2)
Ow1	RbS	0.1639(1)	0.1104(1)	0.1600(2)	0.0248(2)
	CsS	0.1605(1)	0.1088(1)	0.1592(2)	0.0260(2)
	RbSe	0.1635(2)	0.1059(1)	0.1625(2)	0.0246(2)
	CsSe	0.1579(1)	0.1062(1)	0.1591(2)	0.0259(2)
Ow2	RbS	–0.1655(1)	0.1093(1)	0.0275(2)	0.0245(2)
	CsS	–0.1660(1)	0.1069(1)	0.0161(2)	0.0257(2)
	RbSe	–0.1598(2)	0.1081(1)	0.0320(2)	0.0247(2)
	CsSe	–0.1623(1)	0.1051(1)	0.0194(2)	0.0259(2)
Ow3	RbS	0.0012(1)	–0.0652(1)	0.2992(2)	0.0232(2)
	CsS	–0.0014(1)	–0.0635(1)	0.2942(2)	0.0232(2)
	RbSe	–0.0014(2)	–0.0639(1)	0.2928(2)	0.0236(2)
	CsSe	–0.0028(1)	–0.0616(1)	0.2886(2)	0.0239(2)
H11	RbS	0.204(3)	0.091(2)	0.283(4)	0.048(6)
	CsS	0.204(3)	0.099(2)	0.284(4)	0.036(6)
	RbSe	0.202(3)	0.084(2)	0.278(5)	0.032(7)
	CsSe	0.188(3)	0.093(2)	0.263(5)	0.038(7)
H12	RbS	0.230(3)	0.126(2)	0.090(4)	0.040(5)
	CsS	0.221(3)	0.118(2)	0.104(5)	0.040(7)
	RbSe	0.235(4)	0.123(2)	0.124(6)	0.053(9)
	CsSe	0.228(4)	0.122(2)	0.111(5)	0.049(8)
H21	RbS	–0.245(3)	0.098(2)	–0.047(4)	0.037(6)
	CsS	–0.252(3)	0.098(2)	–0.058(4)	0.041(7)
	RbSe	–0.243(4)	0.097(2)	–0.049(5)	0.044(8)
	CsSe	–0.251(3)	0.094(2)	–0.063(5)	0.045(7)
H22	RbS	–0.146(3)	0.165(2)	–0.002(4)	0.040(6)
	CsS	–0.146(3)	0.163(2)	–0.019(4)	0.025(5)
	RbSe	–0.144(4)	0.168(3)	–0.009(5)	0.050(9)
	CsSe	–0.153(3)	0.166(2)	–0.013(5)	0.044(8)

* Tel.: +xx xx 265xxxxx; fax: +xx aa 462xxxxx.
E-mail address: xyz@abc.com.

Table 3 cont.

H31	RbS	–0.074(3)	–0.063(2)	0.333(4)	0.048(6)	
	CsS	–0.074(4)	–0.061(2)	0.336(5)	0.047(8)	
	RbSe	–0.074(4)	–0.055(2)	0.319(5)	0.041(8)	
	CsSe	–0.076(3)	–0.058(2)	0.321(5)	0.041(7)	
H32	RbS	0.021(3)	–0.131(2)	0.328(4)	0.051(6)	
	CsS	0.022(4)	–0.128(3)	0.330(6)	0.071(9)	
	RbSe	0.021(4)	–0.121(3)	0.333(6)	0.058(9)	
	CsSe	0.015(3)	–0.128(2)	0.319(4)	0.034(6)	
HN1	RbS	0.092(12)	0.341(9)	0.214(8)	0.068(21)*	0.198(2)
	RbSe	0.090(6)	0.341(5)	0.222(7)	0.052(9)*	0.496(3)
HN2	RbS	0.211(8)	0.314(8)	0.389(18)	0.068(21)*	0.198(2)
	RbSe	0.213(5)	0.311(4)	0.400(9)	0.052(9)*	0.496(3)
HN3	RbS	0.084(12)	0.319(9)	0.437(16)	0.068(21)*	0.198(2)
	RbSe	0.090(6)	0.318(5)	0.429(9)	0.052(9)*	0.496(3)
HN4	RbS	0.160(13)	0.407(5)	0.417(17)	0.068(21)*	0.198(2)
	RbSe	0.156(7)	0.404(3)	0.380(10)	0.052(9)*	0.496(3)

* H atoms of the NH_4 groups refined with a respective common isotropic displacement parameter

Table 4 lists selected polyhedral bond lengths and angles for structurally investigated single crystals of the ammonium doped Tutton compounds with respective higher bulk ammonium content (x = 0.15), and Table 5 gives relevant data of the respective hydrogen bonding systems. The polyhedral data of the XO_4 (X = S, Se) and NiO_6 units comply very well with general crystal chemical expectations as well as with respective values of the six corresponding endmember structures from literature [1,2,16,38-40] – within these ten compounds, the mean polyhedral bond lengths scatter by a mere 0.006 Å (Ni–O), 0.005 Å (S–O), and 0.002 Å (Se–O). In contrast, as a matter of course, significant differences are observed for the environments of the monovalent cations Rb, Cs, and NH_4^+. Figure 7a-c illustrates the variation of the M–O distances along the $M_{2-y}(NH_4)_yNi(XO_4)_2 \cdot 6H_2O$ (M = Rb, Cs; X = S, Se) solid solution series (Fig. 7b,c) and the resulting changes in lattice parameters (Fig. 7a). Note that y denotes the refined ammonium contents of the investigated single crystals, to be distinguished from the bulk ammonium contents x.

On exchange of Rb by NH_4 groups, the lattice parameters show only minor changes, finally resulting in marginally larger cell volumes in the ammonium endmember compounds (Fig. 7a). However, the Rb/N–O distances clearly reflect the influence of N–H···O hydrogen bonding with increasing ammonium content (Fig. 7b, c): considering the eight nearest oxygen neighbors, the four more distant ones increase their M–O lengths (by averaged 0.052 Å and 0.060 Å in the sulfate and selenate endmembers, respectively), whereas the four closer oxygen atoms are further attracted (by averaged 0.021 Å and 0.024 Å in the sulfate and selenate endmembers, respectively). These closer oxygens (O3, O4, 2×O1; see Table 4) form a distorted tetrahedron and are therefore ideal candidates as acceptors of N–H···O hydrogen bonds of the tetrahedral NH_4 group. This assumption is corroborated by the two cases of our mixed crystals where hydrogen atoms of the NH_4 group could be refined (Table 5), revealing well-defined hydrogen bond geometries with N···O distances between 2.86 and 2.99 Å and N–H···O angles ≥ 145°. From this point of view, orientational disorder of the ammonium ions and the formation of polyfurcate hydrogen bonds are not directly indicated. However, a contribution of the next nearest oxygen neighbor Ow2 as acceptor can not be ruled out completely; in case of the

* Tel.: +xx xx 265xxxxx; fax: +xx aa 462xxxxx.
E-mail address: xyz@abc.com.

ammonium-rich rubidium selenate (y = 0.99), the significant negative deviation from a linear M–O trend (Fig. 7c) might hint at such a contribution.

Table 4. Bond lengths (Å) and angles (°) for select ed single crystals (see text) of ammonium-doped Tutton compounds $M_{2-y}(NH_4)_yNi(XO_4)_2 \cdot 6H_2O$ (M = Rb, Cs; X = S, Se). Estimated standard deviations are 1 in the last digit (else otherwise stated)

MX	RbS	CsS	RbSe	CsSe
refined y (NH_4)	0.395(4)	0.275(4)	0.991(5)	0.259(3)
X–O2	1.464	1.466	1.623	1.631
X–O1	1.474	1.475	1.638	1.636
X–O3	1.477	1.480	1.638	1.642
X–O4	1.481	1.483	1.643	1.644
<X–O>	1.474	1.476	1.636	1.638
O2–X–O1	109.8	110.2	109.4	109.8
O2–X–O3	108.7	108.6	108.4	108.5
O2–X–O4	110.7	110.8	111.3	111.4
O1–X–O3	108.3	108.5	107.8	108.0
O1–X–O4	109.6	109.4	109.5	109.4
O3–X–O4	109.7	109.4	110.3	109.8
Ni–Ow3 2×	2.030	2.039	2.032	2.035
Ni–Ow1 2×	2.071	2.065	2.077	2.071
Ni–Ow2 2×	2.076	2.078	2.070	2.075
<Ni–O>	2.056	2.061	2.059	2.060
Ow3–Ni–Ow1 2×	90.3	90.9	89.2	89.8
Ow3–Ni–Ow1’ 2×	89.7	89.1	90.8	90.2
Ow3–Ni–Ow2 2×	90.1	89.4	89.2	90.0
Ow3–Ni–Ow2’ 2×	89.9	90.6	90.8	90.0
Ow1–Ni–Ow2 2×	88.5	88.5	88.6	88.7
Ow1–Ni–Ow2’ 2×	91.5	91.5	91.4	91.3
M,N–O3	2.860	3.026	2.856(2)	3.030(2)
M,N–O4	2.931	3.071(2)	2.924(2)	3.084(2)
M,N–O1	2.979	3.099(2)	2.985(2)	3.109(2)
M,N–O1	2.992	3.071(2)	2.962(2)	3.060(2)
M,N–Ow2	3.122	3.297	3.152	3.306
M,N–O2	3.150	3.306(2)	3.258(2)	3.383(2)
M,N–O2	3.228	3.279(2)	3.362(2)	3.362(2)
M,N–Ow1	3.238	3.399	3.249(2)	3.405
M,N–O2	3.533	3.480(2)	3.636(2)	3.574(2)
M,N–Ow3	3.617	3.657	3.712(2)	3.761
$<M,N–O>^{[4]}$	2.940	3.066	2.932	3.071
$<M,N–O>^{[8]}$	3.062	3.193	3.094	3.217
$<M,N–O>^{[9]}$	3.115	3.225	3.154	3.257
$<M,N–O>^{[10]}$	3.165	3.268	3.210	3.307

* Tel.: +xx xx 265xxxxx; fax: +xx aa 462xxxxx.
E-mail address: xyz@abc.com.

On exchange of Cs by NH_4 groups, the lattice parameters clearly decrease as a consequence of the smaller space requirements of the ammonium groups (Fig. 7a). Likewise, the Cs/N–O distances show quite severe changes: of the eight nearest oxygen neighbors, seven decrease their distance at a quite strong and similar rate (by averaged 0.157 Å along the full solid solution series), only the Cs/N–O2 distance moderately increases (Fig. 7b ,c). The four closer oxygen atoms are again in a pseudo-tetrahedral arrangement, and the gap to the four longer Cs/N–O distances is always larger compared to the respective rubidium-containing compounds. This argues against orientational disorder of the ammonium ions or the formation of polyfurcate N–H···O hydrogen bonds in the cesium salt matrices. But on the other hand, at the comparatively low ammonium contents present in the structurally investigated cesium mixed crystals (y = 0.17-0.28), strong local distortions of the oxygen environments, possibly combined with positional disorder of the ammonium ions, are likely to occur, which are not readily detectable by long-range diffraction methods.

Table 5. Hydrogen bond lengths (Å) and angles (°) f or selected single crystals (see text) of ammonium-doped Tutton compounds $M_{2-y}(NH_4)_yNi(XO_4)_2 \cdot 6H_2O$ (M = Rb, Cs; X = S, Se)

MX	RbS	CsS	RbSe	CsSe
refined y (NH_4)	0.395(4)	0.275(4)	0.991(5)	0.259(3)
Ow1–H11	0.79(2)	0.78(3)	0.77(3)	0.68(3)
Ow1–H12	0.86(2)	0.75(3)	0.80(3)	0.83(3)
Ow1···O3	2.758(2)	2.744(2)	2.789(2)	2.769(2)
Ow1···O4	2.802(2)	2.796(2)	2.828(2)	2.798(2)
Ow1–H11···O3	167(2)	168(3)	164(3)	170(3)
Ow1–H12···O4	173(2)	165(3)	167(4)	167(3)
Ow2–H21	0.76(2)	0.80(3)	0.81(3)	0.87(3)
Ow2–H22	0.75(2)	0.79(2)	0.83(3)	0.82(3)
Ow2···O2	2.698(2)	2.724(2)	2.686(2)	2.714(2)
Ow2···O4	2.748(2)	2.754(2)	2.750(2)	2.757(2)
Ow2–H21···O2	176(2)	172(3)	175(3)	171(3)
Ow2–H22···O4	170(2)	163(2)	166(3)	169(3)
Ow3–H31	0.77(2)	0.79(3)	0.75(3)	0.77(3)
Ow3–H32	0.85(2)	0.87(3)	0.78(4)	0.89(3)
Ow3···O3	2.746(1)	2.760(2)	2.753(2)	2.756(2)
Ow3···O1	2.680(1)	2.682(2)	2.708(2)	2.684(2)
Ow3–H31···O3	173(2)	168(3)	169(3)	170(3)
Ow3–H32···O1	174(2)	176(4)	178(4)	172(3)
N–HN1	0.82(4)		0.80(4)	
N–HN2	0.83(4)		0.79(4)	
N–HN3	0.88(4)		0.85(4)	
N–HN4	0.83(4)		0.80(4)	
N···O4	2.931(1)		2.924(2)	
N···O1	2.992(1)		2.962(2)	
N···O1	2.979(1)		2.985(2)	
N···O3	2.860(1)		2.856(2)	
N–HN1···O4	148(11)		153(6)	
N–HN2···O1	164(10)		174(6)	
N–HN3···O1	164(11)		167(6)	
N–HN4···O3	145(10)		163(6)	

* Tel.: +xx xx 265xxxxx; fax: +xx aa 462xxxxx.
E-mail address: xyz@abc.com.

The hydrogen bonding system involving the three different water molecules is also affected to some extent by the replacement of Rb or Cs by NH_4^+ groups. In the alkali endmembers [1,2,39,40], the moderately strong Ow···O hydrogen bonds range between ~2.67 to ~2.80 Å. With the only significant exception of Ow2···O2 in the cesium compounds, the other hydrogen bonds to O1, O3 and O4 tend to become longer and thus weaker (or remain roughly constant) with increasing ammonium content. This behavior can be readily explained due to the additional participation of O1, O3 and O4 as acceptors in N–H···O hydrogen bonds of the ammonium ions in the mixed crystals and in the NH_4 endmember compounds.

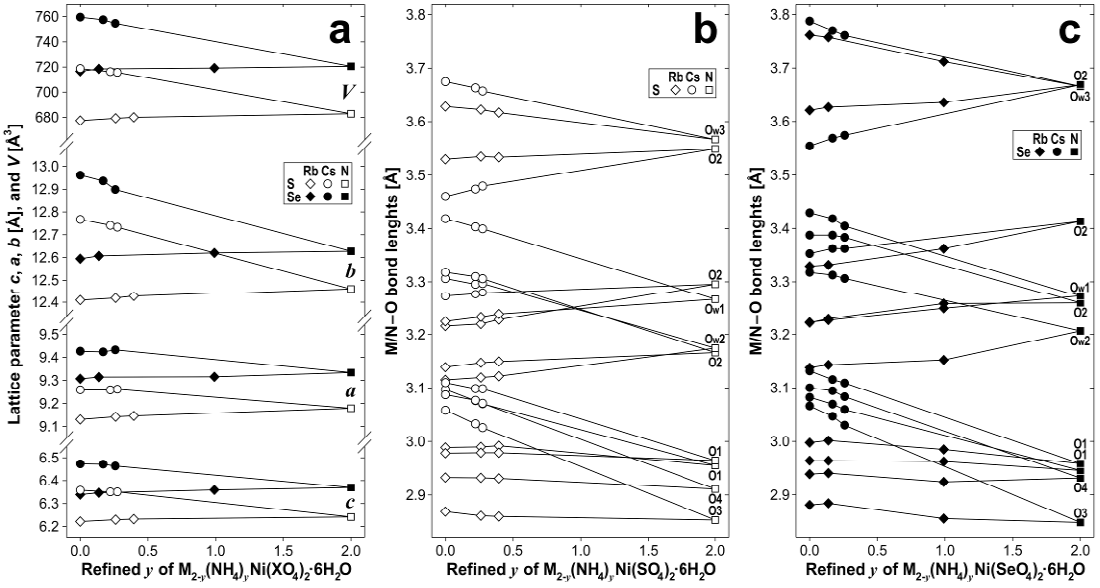

Fig. 7. Changes in lattice parameters (a) and variation of the M/N–O distances along the $M_{2-y}(NH_4)_yNi(XO_4)_2 \cdot 6H_2O$ (M = Rb, Cs; X = S, Se) solid solution series (b, sulfates; c, selenates). Data for the endmember compositions are taken from Refs. [1,2,16,38-40]

2. CONCLUSIONS

(i) A double salt, $Cs_2Ni(SO_4)_2 \cdot 6H_2O$, crystallizes from the ternary Cs_2SO_4−$NiSO_4$−H_2O system within a wide concentration range.

(ii) The ammonium ions isomorphously included in the cesium and rubidium sulfates exhibit three bands corresponding to the asymmetric bending modes ν_4 in agreement with the low site symmetry C_1 of the host cesium and rubidium ions. However, the inclusion of ammonium ions in the selenate matrices leads to the appearance of four bands in the region of ν_4 due to some kind of disorder of the ammonium ions. This phenomenon is probably due to the stronger proton acceptor ability of the selenate ions.

(iii) The hydrogen bonds formed in the $M_{1.85}(NH_4)_{0.15}Ni(XO_4)_2 \cdot 6H_2O$ (M = Rb, Cs; X = S, Se) mixed crystals as deduced from the wavenumbers of the water librations are weaker as compared to those formed in the neat rubidium and cesium compounds. The formation of hydrogen bonds between the ammonium guest cations and the host anions leads to the decrease in the proton acceptor capacity of the SO_4^{2-} and SeO_4^{2-} anions (*anti*-cooperative or proton acceptor competitive effect).

* Tel.: +xx xx 265xxxxx; fax: +xx aa 462xxxxx.
E-mail address: xyz@abc.com.

(iv) Single crystal structure investigations of $(M,NH_4)_2Ni(XO_4)_2 \cdot 6H_2O$ (M = Rb, Cs; X = S, Se) mixed crystals show significant changes in the environment of the monovalent cations upon incorporation of ammonium ions. Likewise, the weakening of hydrogen bonds of the water molecules, revealed by infrared spectroscopy, is confirmed by increasing Ow···O hydrogen bond lengths. Disorder of NH_4 groups or the formation of polyfurcate N–H···O hydrogen bonds have not been observed in the diffraction experiments, but can not be excluded, especially not for low ammonium contents.

ACKNOWLEDGEMENTS

The financial support of the National Science Fund of Republic of Bulgaria (project BG051PO001/3.3-05-0001) is gratefully acknowledged.

COMPETING INTERESTS

Authors have declared that no competing interests exist.

AUTHORS' CONTRIBUTIONS

This work was carried out in collaboration between all authors. Author MW performed and interpreted single crystal X-ray diffraction measurements and wrote the part for the structural data. Author DS interpreted and wrote the part concerning the infrared spectroscopic measurements. Author VK performed experiments: preparation of the samples, X-ray diffraction and infrared spectroscopic measurements. VK participated in discussions of experimental results as well. All authors read and approved the final manuscript.

REFERENCES

1. Euler H, Barbier B, Meents A, Kirfel A. Crystal structure of Tutton's salts, $Cs_2[M^{II}(H_2O)_6](SeO_4)_2$, M^{II} = Mg, Mn, Co, Ni, Zn. Z Kristallogr NCS. 2003:218(4):405-408.
Available: DOI: 10.1524/ncrs.2003.218.4.405.
2. Euler H, Barbier B, Meents A, Kirfel A. Crystal structure of Tutton's salts, $Cs_2[M^{II}(H_2O)_6](SO_4)_2$, M^{II} = Mg, Mn, Fe, Co, Ni, Zn. Z Kristallogr NCS. 2003:218(4):409-413.
Available: DOI: 10.1524/ncrs.2003.218.4.409.
3. Marinova D, Georgiev M, Stoilova D. Vibrational behavior of matrix-isolated ions in Tutton compounds. I. Infrared Spectroscopic study of NH_4^+ and SO_4^{2-} ions included in magnesium sulfates and selenates. J Mol Struct. 2009:929(1-3):67-72.
Available: DOI: 10.1016/j.molstruc.2009.04.004.
4. Marinova D, Georgiev M, Stoilova D. Vibrational behavior of matrix-isolated ions in Tutton compounds. II. Infrared spectroscopic study of NH_4^+ and SO_4^{2-} ions included in copper sulfates and selenates. J Mol Struct. 2009:938(1-3):179-184.
Available: DOI: 10.1016/j.molstruc.2009.09.023.
5. Marinova D, Georgiev M, Stoilova D. Vibrational behavior of matrix-isolated ions in Tutton compounds. V. Infrared spectroscopic study of NH_4^+ and SO_4^{2-} ions included in zinc sulfates and selenates. Solid State Sci. 2010:12(5):765-769.
Available: DOI: 10.1016/j.solidstatesciences.2010.02.02.
6. Georgiev M, Marinova D, Stoilova D. Vibrational behavior of matrix-isolated ions in Tutton compounds. III. Infrared spectroscopic study of NH_4^+ and SO_4^{2-} ions included in cobalt sulfates and selenates. Vibr Spectrosc. 2010:53:233-238.
Available: DOI: 10.1016/j.vibspec.2010.03.014.

* Tel.: +xx xx 265xxxxx; fax: +xx aa 462xxxxx.
E-mail address: xyz@abc.com.

7. Marinova D, Georgiev M, Stoilova D, Vibrational behavior of matrix-isolated ions in Tutton compounds. IV. Infrared spectroscopic study of NH_4^+ and SO_4^{2-} ions included in nickel sulfates and selenates, Cryst. Res. Technol. 2010:45:637-642.
Available: DOI:10.1002/crat.200900668.
8. Karadjova V, Stoilova D. Infrared spectroscopic study of $Rb_2M(XO_4)_2 \cdot 6H_2O$ (M = Mg, Co, Ni, Cu, Zn; X = S, Se) and of SO_4^{-2} guest ions included in rubidium Tutton selenates. J Mol Struct. 2013:1050:204-210.
Available: DOI: 10.1016/j.molstruc.2013.07.013.
9. Karadjova V, Stoilova D. Crystallization in the three-component systems Rb_2SO_4–$MeSO_4$–H_2O (Me = Mg, Co, Ni, Cu, Zn) at 25 °C. J Cryst Proc Technol. 2013:3(3):136-147.
Available: http://dx.doi.org/10.4236/jcpt.2013.34022.
10. Karadjova V. Crystallization in the three-component systems Rb_2SeO_4–$MeSeO_4$–H_2O (Me = Mg, Ni, Cu) at 25 °C. J Univ Chem Technol Metal (Sofia). 2013:48(3):316-325.
11. Oikova T, Barkov D, Popov A. Untersuchung der Phasengleichgewichte in den Systemen Cs_2SeO_4–$CoSeO_4$–H_2O und Cs_2SeO_4–$NiSeO_4$–H_2O bei 25.0℃. Monatsh Chem. 2000:131(7):727-732.
Available: DOI: 10.1007/s007060070073.
12. Balarew Chr, Karaivanova V, Oikova T. Beitrag zur Untersuchung der isomorphen und isodimorphen Einschluesse in Kristallsalzen. III. Untersuchung der Systeme Zinksulfat-Kobaltsulfat-Wasser und Zinksulfat-Nickelsulfat-Wasser bei 25 ℃. Commun Departm Chem. Bulg Acad Sci. 1970:3(4):673-644.
13. Nonius, Kappa CCD program package, Nonius B.V. Delft 1998.
14. Sheldrick GM. A short history of SHELX. Acta Crystallogr. 2008:A64(1):112-122.
Available: DOI: 10.1107/S0108767307043930.
15. Bosi F, Belardi G, Ballirano P. Structural features in Tutton's salts $K_2[M^{2+}(H_2O)_6](SO_4)_2$, with M^{2+} = Mg, Fe, Co, Ni, Cu, and Zn. Amer Mineralogist. 2009:94(1):74-82.
16. Montgomery H. Diammonium nickel diselenate hexahydrate, Acta Crystallogr. 1980:B36(2):440-442.
Available: DOI: 10.1107/S0567740880003445.
17. Nakamoto K. Infrared and Raman Spectra of Inorganic and Coordination Compounds, John Wiley & Sons New York 1986.
18. Brown RG, Ross SD. Forbidden transitions in the infrared spectra of tetrahedral anions–VI. Tutton salts and other double sulfates and selenates Spectrochim Acta. 1970:26A(4):945-953.
19. Gampbell JA, Ryan DP, Simpson LM. Interionic forces in crystal – II. Infrared spectra of SO_4 groups and "octahedrally" coordinated water in some Alums, Tutton salts, and the double salts obtained by dehydrating them. Spectrochim Acta. 1970:26A(12):2351-2361.
20. Petruševski V, Šoptrajanov B. Description of molecular distortions II. Intensities of the symmetric stretching bands of tetrahedral molecules. J Mol Struct. 1988:175:349-354.
Available: DOI: 10.1016/S0022-2860(98)80101-4.
21. Petruševski VM, Šoptrajanov B. Infrared spectra of the dihydrates of calcium selenate and yttrium phosphate - comparison with the spectrum of gypsum. J Mol Struct. 1984:115:343-346.
Available: DOI: 10.1016/0022-2860(84)80084-8.
22. Šoptrajanov B, Petruševski VM. Infrared spectra of Li_2SeO_4, $Li_2SeO_4 \cdot H_2O$ and Li_2 (S,Se) $O_4 \cdot H_2O$. J Mol Struct. 1986:142:67-70.
Available: DOI: 10.1016/0022-2860(86)85064-5.
23. Lutz HD. Bonding and structure of water molecules in solid hydrates. Correlation of spectroscopic and structural data. Struct Bond (Berlin). 1988:69:97-123.
24. Stoilova D, Lutz HD. Infrared study of ν_{OD} modes in isotopically dilute (HDO) kieserite-type compounds $MXO_4.H_2O$ (M = Mn, Co, Ni, Zn, and X = S, Se) with matrix-isolated M'^{2+} and $X'O_4^{2-}$ guest ions. J Mol Struct.1998:450(1-3):101-106.

* Tel.: +xx xx 265xxxxx; fax: +xx aa 462xxxxx.
E-mail address: xyz@abc.com.

Available: DOI: 10.1016/S0022-2860(98)90417-3.
25. Lutz HD, Engelen B. Hydrogen bonds in inorganic solids. Trends Appl Spectrosc. 2002:4:355-375.
26. Stoilova D, Wildner M, Koleva V. Infrared study of ν_{OD} modes in isotopically dilute (HDO molecules) $Na_2Me(XO_4)_2 \cdot 2H_2O$ with matrix-isolated $X'O_4^{2-}$ guest ions (Me = Mn, Co, Ni, Cu, Zn, Cd, and X = S, Se). J Mol Struct. 2002:643(1-3):37-41.
Available: DOI: 10.1016/S0022-2860(02)00404-0.
27. Lutz HD. Structure and strength of hydrogen bonds in inorganic compounds. J Mol Struct. 2003:646(1-3):227-236.
Available: DOI: 10.1016/S0022-2860(02)00716-0.
28. Šoptrajanov B, Petruševski VM. Vibrational spectra of hexaaqua complexes V. The water bending bands in the infrared spectra of Tutton salts. J Mol Struct. 1997:408/409:283-286.
Available: DOI: 10.1016/S0022-2860(96)09660-3.
29. Ebert M, Vojtišek P. The hydrates of double selenates. Chem papers 1993:47(5):292-296.
30. Mička Zd, Prokopová L, Cisařová I, Havliček D. Crystal structure, thermoanalytical properties and infrared spectra of double magnesium selenates. Collect Czech Chem Commun. 1996:61(9):1295-1306.
Available: http://dx.doi.org/10.1135/cccc19961295.
31. Vojtišek P, Ebert M. Löslichkeitsuntersuchung in den Systemen Rb_2SeO_4-$MgSeO_4$-H_2O und Cs_2SeO_4-$MgSeO_4$-H_2O bei 25ºC. Z Chem. 1987:27(7):266-267.
Available: DOI: 10.1002/zfch.19870270715.
32. Fleck M, Kolitsch U. Crystal structure of ammonium hexaaquacobalt(II) selenate, $(NH_4)_2[Co(H_2O)_6](SeO_4)_2$, and hexaaquazinc selenate, $(NH_4)_2[Zn(H_2O)_6](SeO_4)_2$, hydrogen bonds in two ammonium selenate Tutton's salts. Z Kristallogr NCS. 2002:217(JG):471-473.
Available: DOI: 10.1524/ncrs.2002.217.jg.471.
33. Khan AA, Baur WH. Salt hydrates. VIII. The crystal structures of sodium ammonium orthochromate dihydrate and magnesium diammonium bis(hydrogen orthophosphate) tetrahydrate and a discussion of the ammonium ion. Acta Crystallogr. 1972:B28(3):683-693.
DOI: 10.1107/S0567740872003024.
34. Cahil A, Najdovski M, Stefov V. Infrared and Raman spectra of magnesium ammonium phosphate hexahydrate (struvite) and its isomorphous analogues. IV. FTIR spectra of protiated and partially deuterated nickel ammonium phosphate hexahydrate and nickel potassium phosphate hexahydrate. J. Mol. Struct. 2007:834/836:408-413.
Available: DOI: 10.1016/j.molstruc.2006.11.049.
35. Stefov V, Šoptrajanov B, Kuzmanovski I, Lutz HD, Engelen B. Infrared and Raman spectra of magnesium ammonium phosphate hexahydrate (struvite) and its isomorphous analogues. III. Spectra of protiated and partially deuterated magnesium ammonium phosphate hexahydrate. J Mol Struct. 2005:752(1-3):60-67.
Available: DOI: 10.1016/j.molstruc.2005.05.040.
36. Stefov V, Šoptrajanov B, Najdovski M, Engelen B, Lutz HD. Infrared and Raman spectra of magnesium ammonium phosphate hexahydrate (struvite) and its isomorphous analogues. V. Spectra of protiated and partially deuterated magnesium ammonium arsenate hexahydate (arsenstruvite). J Mol Struct. 2008:872(2-3):87-92.
Available: DOI: 10.1016/j.molstruc.2007.02.017.
37. Cahil A, Šoptrajanov B, Najdovski M, Lutz HD, Engelen B, Stefov V. Infrared and Raman spectra of magnesium ammonium phosphate hexahydrate (struvite) and its isomorphous analogues. Part VI: FT-IR spectra of isomorphously isolated species. NH_4^+ ions isolated in $MKPO_4 \cdot 6H_2O$ (M = Mg, Ni) and PO_4^{3-} ions isolated in $MgNH_4AsO_4 \cdot 6H_2O$. J Mol Struct. 2008:876(1-3):255-259.
Available: DOI: 10.1016/j.molstruc.2007.06.023.

* Tel.: +xx xx 265xxxxx; fax: +xx aa 462xxxxx.
E-mail address: xyz@abc.com.

38. Maslen EN, Ridout SC, Watson KJ, Moore FH. The structures of Tutton's salts. II. Diammonium hexaaquanickel(II) sulfate. Acta Crystallogr. 1988:C44(3):412-415. Available: DOI: 10.1107/S0108270187009995.
39. Fleck M, Kolitsch U. Crystal structure of the Tutton's salts rubidium hexaaquanickel(II) selenate, $Rb_2[Ni(H_2O)_6](SeO_4)_2$, and rubidium hexaaquacopper(II) selenate, $Rb_2[Cu(H_2O)_6](SeO_4)_2$. Z Kristallogr NCS. 2002:217(JG):15-16. Available: DOI:10.1524/ncrs.2002.217.jg.15,
40. Euler H, Barbier B, Klumpp S, Kirfel A. Crystal structure of Tutton's salts, $Rb_2[M^{II}(H_2O)_6](SO_4)_2$, M^{II} = Mg, Mn, Fe, Co, Ni, Zn. Z Kristallogr NCS. 2000:215(4):473-476.

* Tel.: +xx xx 265xxxxx; fax: +xx aa 462xxxxx.
E-mail address: xyz@abc.com.